

Effective Lagrangians and low energy photon-photon scattering

Duane A. Dicus¹, Chung Kao² and Wayne W. Repko³

¹*Center for Particle Physics and Department of Physics,
University of Texas, Austin, Texas 78712*

²*Department of Physics, University of Wisconsin, Madison, Wisconsin 53706*

³*Department of Physics and Astronomy,
Michigan State University, East Lansing, Michigan 48824*

(December 2, 2024)

Abstract

We investigate the behavior of the photon-photon scattering near the threshold $\omega = m_e$, by comparing the exact result with the approximation obtained using the Euler-Heisenberg effective Lagrangian supplemented with higher-order derivative corrections. We also examine the ω^2/m_e^2 behavior predicted by including one-loop corrections to the Euler-Heisenberg effective Lagrangian together with the necessary counterterms. At the one-loop level, it is not possible to reproduce the ω^2/m_e^2 dependence of QED by simply using the Euler-Heisenberg expansion.

11.10.Ge,14.70.Bh,21.30.Fe

I. INTRODUCTION

Photon–photon scattering is tedious to calculate and, in general, the final expression involves many Spence functions which must be evaluated numerically [1,2]. The exception occurs when the photon energy, ω , is small compared to the electron mass. In this limit the amplitudes take on a simple analytic form (see below) and the cross section for unpolarized radiation is given by the well known expression [3]

$$\frac{d\sigma}{d\Omega} = \frac{\alpha^4}{(180\pi)^2} 139 (3 + z^2)^2 \frac{\omega^6}{m_e^8}, \quad (1)$$

where z is the cosine of the scattering angle and m_e is the mass of the electron. There is no particular reason to expect this cross section to remain valid as ω approaches m_e but a plot of the full cross section, as in Fig. 1, shows that the straight, ω^6 , behavior does hold at least up to $\omega \simeq 0.4 m_e$ or so. Figure 1 also shows that the slope increases as ω approaches m_e which implies that still higher powers of ω/m_e are contributing. Our purpose here is to investigate the usefulness of Eq. (1) as ω approaches m_e , to explore the extent to which adding more terms to the cross section expansion in powers of ω/m_e improves the agreement between the exact numerical and simple analytic results, to determine the structure of the effective interactions which give these corrections, and to compare these interactions with the higher order contributions obtained from the Euler-Heisenberg interaction which gives Eq. (1).

In Section II, we give the helicity amplitudes which result from expanding the electron box diagrams in powers of ω^2/m_e^2 . We also display an effective Lagrangian which generalizes the Euler-Heisenberg Lagrangian and reproduces the QED expansion. In Section III, we derive the one-loop corrections to low energy photon-photon scattering using the Euler-Heisenberg effective Lagrangian. This is followed by a discussion comparing photon-photon amplitudes obtained in the preceding two Sections.

II. A GENERALIZED EFFECTIVE LAGRANGIAN

The ω^6 dependence of the low energy cross section follows from the fact that the only independent, parity conserving gauge invariant interactions for photon–photon scattering involving only the photon fields are $F_{\mu\nu}F^{\mu\nu}F_{\lambda\rho}F^{\lambda\rho}$ and $F_{\mu\nu}F^{\nu\lambda}F_{\lambda\rho}F^{\rho\mu}$. The Euler-Heisenberg interaction is a particular combination of these forms (see Eq. (8)). Thus, the amplitudes go as ω^4 and, using QED or Eq. (8), the helicity amplitudes are given by [1]

$$T_{++++}^4(z) = -\frac{176}{45} \alpha^2 \frac{\omega^4}{m_e^4} \quad (2a)$$

$$T_{++--}^4(z) = \frac{8}{15} \alpha^2 \frac{\omega^4}{m_e^4} (3 + z^2) \quad (2b)$$

$$T_{+-+-}^4(z) = -\frac{44}{45} \alpha^2 \frac{\omega^4}{m_e^4} (1 + z)^2 = T_{+--+}^4(-z) \quad (2c)$$

$$T_{++++}^4(z) = T_{+--+}^4(z) = 0, \quad (2d)$$

with the remaining amplitudes equal to these by parity and time reversal. Equation (1) follows by taking the sum of the squares of Eqs. (2).

Table I compares the total cross section, as calculated approximately by integrating Eq. (1) over z ,

$$\sigma = \frac{1}{(45)^2} \frac{973}{5} \frac{\alpha^4}{\pi} \frac{\omega^6}{m_e^8}, \quad (3)$$

with the full one loop expression calculated by using a rapidly converging series for the Spence functions [4] and performing a numerical integration over z . As can be seen, Eq. (3) provides a reasonable approximation for $\omega/m_e \lesssim 0.50$. We have also compared the differential cross section for explicit values of z . The Euler cross section Eq. (1) is within 10% of the true differential cross section for $\omega/m_e \lesssim 0.45$ for the worst case which is right angle scattering.

Corrections to Eqs. (1) or (3) can only involve effective interactions with derivatives acting on four factors of $F_{\mu\nu}$ and, by Lorentz invariance, must involve an even number of derivatives. Thus the helicity amplitudes and therefore the cross section are expansions in ω^2/m_e^2 . We have calculated the terms of order ω^6 and ω^8 by expanding the electron box diagrams of QED. The amplitudes of order $\alpha^2\omega^6/m_e^6$ are

$$T_{++++}^6(z) = -\frac{768}{945} \quad (4a)$$

$$T_{++--}^6(z) = \frac{480}{945} (1 - z^2) \quad (4b)$$

$$T_{+--+}^6(z) = \frac{96}{945} (1 + z)^3 = T_{+--+}^6(-z) \quad (4c)$$

$$T_{++++}^6(z) = T_{+--+}^6(z) = \frac{48}{945} (1 - z^2), \quad (4d)$$

and for those of order $\alpha^2\omega^8/m_e^8$, we find

$$T_{++++}^8(z) = -\frac{64}{4725} (157 + 25 z^2) \quad (5a)$$

$$T_{++--}^8(z) = \frac{640}{4725} (3 + z^2)^2 \quad (5b)$$

$$T_{+--+}^8(z) = -\frac{8}{4725} (1 + z)^2 (191 + 82 z + 91 z^2) \quad (5c)$$

$$T_{+--+}^8(z) = T_{+--+}^8(-z) \quad (5d)$$

$$T_{++++}^8(z) = T_{+--+}^8(z) = 0. \quad (5e)$$

These amplitudes add terms to Eq. (1) which becomes

$$\begin{aligned} \frac{d\sigma}{d\Omega} = \frac{\alpha^4}{(180\pi)^2} \frac{\omega^6}{m_e^8} \left\{ 139 (3 + z^2)^2 + 160 \frac{\omega^2}{m_e^2} (1 - z^2)(3 + z^2) + \frac{4}{7} \frac{\omega^4}{m_e^4} \left[\frac{16}{7} (46 - 11 z^2 \right. \right. \\ \left. \left. + 28 z^4 + z^6) + \frac{11}{35} (2703 + 1965 z^2 + 1065 z^4 + 91 z^6) + 16 (3 + z^2)^3 \right] \right\}, \quad (6) \end{aligned}$$

where the first term is the contribution from the square of the ω^4 amplitude (Eq. (1)), the second term is the cross term between the amplitudes of order ω^4 with those of order ω^6 (given by Eqs. (2) and (4)), the third term is the square of the ω^6 amplitudes, and the last two come from the cross terms between the ω^4 amplitudes and those of order ω^8 . The corresponding total cross section is

$$\sigma = \frac{1}{(45)^2} \frac{\alpha^4 \omega^6}{\pi m_e^8} \left\{ \frac{973}{5} + \frac{128}{3} \frac{\omega^2}{m_e^2} + \frac{409792}{1715} \frac{\omega^4}{m_e^4} \right\}. \quad (7)$$

The last column of Table I gives the ratio of Eq. (7) to the full one loop cross section. Inclusion of the second and third terms in Eq. (7) provides a very good approximation, all the way to $\omega/m_e \simeq 0.90$. Again, a comparison of Eq. (6) with the true differential cross section reveals a difference of less than 10% for $\omega < 0.85m_e$ at any scattering angle. There are also contributions of order $\alpha^5 \omega^4/m_e^4$ arising from the one-loop corrections to the box diagram [5]. This effect multiplies Eqs. (1), (3) and the $973/5$ term of (7) by $[1 + (186685/17514)(\alpha/\pi)]$. The corrections we discuss exceed this correction when $\omega/m_e > 0.28$.

It is well known [3] that the helicity amplitudes, Eqs. (2), can be obtained from the effective Lagrangian

$$\mathcal{L}_{\text{eff}} = \frac{1}{180} \frac{\alpha^2}{m_e^4} \left\{ 5 (F_{\mu\nu} F^{\mu\nu})^2 - 14 F_{\mu\nu} F^{\nu\lambda} F_{\lambda\rho} F^{\rho\mu} \right\}. \quad (8)$$

In order to generalize this expression to reproduce the ω^6 and ω^8 corrections, it is necessary to construct terms containing two or four additional derivatives acting on a combination of four $F_{\mu\nu}$'s to produce a scalar. Doing so is something of a trial and error process. There are many tensors which can be formed with the required properties, but most of them are not independent. The forms given below are sufficient to reproduce the helicity amplitudes of Eqs. (4) and (5). For the ω^6 correction, we find

$$\begin{aligned} \mathcal{L}'_{\text{eff}} = \frac{1}{945} \frac{\alpha^2}{m_e^6} \left\{ (\partial^\alpha \partial_\beta F_{\mu\nu}) F^{\mu\nu} F_{\alpha\lambda} F^{\lambda\beta} + 3 (\partial^\alpha F_{\mu\nu}) (\partial_\alpha F^{\mu\nu}) F_{\lambda\rho} F^{\lambda\rho} \right. \\ \left. + 11 (\partial^\alpha F_{\mu\nu}) F^{\nu\lambda} (\partial_\alpha F_{\lambda\rho}) F^{\rho\mu} \right\}. \end{aligned} \quad (9)$$

The ω^8 correction is given by

$$\begin{aligned} \mathcal{L}''_{\text{eff}} = -\frac{1}{9450} \frac{\alpha^2}{m_e^8} \left\{ 33 (\partial_\alpha F_{\mu\nu}) (\partial^\alpha F^{\mu\nu}) (\partial_\beta F_{\lambda\rho}) (\partial^\beta F^{\lambda\rho}) \right. \\ \left. - 106 (\partial_\alpha F_{\mu\nu}) (\partial^\beta F^{\mu\nu}) (\partial^\alpha F_{\lambda\rho}) (\partial_\beta F^{\lambda\rho}) + 262 (\partial^\alpha \partial_\beta F_{\mu\lambda}) F^{\lambda\nu} (\partial^\mu \partial_\nu F_{\alpha\rho}) F^{\rho\beta} \right\}. \end{aligned} \quad (10)$$

The expansion of the photon-photon scattering amplitude can thus be obtained by computing the matrix element of the local effective Lagrangian $\mathcal{L}_{\text{eff}} + \mathcal{L}'_{\text{eff}} + \mathcal{L}''_{\text{eff}}$.

III. ONE-LOOP CORRECTIONS

The expansion derived in the previous section is a specific example of how the low energy behavior of a renormalizable field theory can be explored by 'integrating out' the

heavy degrees of freedom to obtain an effective interaction. In fact, there are compelling arguments which suggest that effective field theories are adequate descriptions of Nature if one accepts a reasonable set of assumptions about the renormalization program [6]. To explore this approach for low energy photon-photon scattering, we calculate the one-loop corrections generated by the Euler-Heisenberg Lagrangian [7]. For a one-loop calculation, it suffices to use the terms [8]

$$\begin{aligned} \mathcal{L}_{\text{E-H}} = & \frac{1}{180} \frac{\alpha^2}{m_e^4} \left\{ 5 (F_{\mu\nu} F^{\mu\nu})^2 - 14 F_{\mu\nu} F^{\nu\lambda} F_{\lambda\rho} F^{\rho\mu} \right\} \\ & + \frac{1}{315} \frac{\pi \alpha^3}{m_e^8} \left\{ 9 (F_{\mu\nu} F^{\mu\nu})^3 - 26 F_{\mu\nu} F^{\nu\lambda} F_{\lambda\rho} F^{\rho\mu} F_{\alpha\beta} F^{\alpha\beta} \right\}. \end{aligned} \quad (11)$$

The one-loop contribution of the order α^3 term in Eq. (11) to the photon-photon scattering amplitude, obtained by contracting a pair of $F_{\mu\nu}$'s, actually vanishes by dimensional regularization [9]. This leaves only the α^4 one-loop contribution from the first term of Eq. (11) used in the second order of perturbation theory. Because the photons are massless, all the loop integrals, which take the form

$$B_{\alpha_1 \dots \alpha_i} = \frac{1}{i\pi^2} \int d^4 q \frac{q_{\alpha_1} \dots q_{\alpha_i}}{q^2 (q+k)^2}, \quad (12)$$

$i = 1, \dots, 4$, are proportional to the scalar integral

$$B_0(k^2) = \frac{1}{i\pi^2} \int d^4 q \frac{1}{q^2 (q+k)^2}, \quad (13)$$

multiplied by a polynomial in the momentum k . Evaluating $B_0(k^2)$ using a cutoff Λ , we find

$$B_0(k^2) = \ln \left(\frac{\Lambda^2}{-k^2 - i\varepsilon} \right). \quad (14)$$

In second order, the α^2 term in Eq. (11) has s , t and u channel contributions, illustrated in Fig. 2. As a consequence, the one-loop correction to the helicity amplitudes can be written

$$T_{\lambda_1 \lambda_2 \lambda_3 \lambda_4}^{(2)} = \frac{\alpha^4}{(45\pi)^2} \frac{\omega^8}{m_e^8} \left(T_{\lambda_1 \lambda_2 \lambda_3 \lambda_4}^s B_0(s) + T_{\lambda_1 \lambda_2 \lambda_3 \lambda_4}^t B_0(t) + T_{\lambda_1 \lambda_2 \lambda_3 \lambda_4}^u B_0(u) \right), \quad (15)$$

with $s = (k_1 + k_2)^2$, $t = (k_1 - k_3)^2$ and $u = (k_1 - k_4)^2$. Since the vertex functions resulting from $\mathcal{L}_{\text{E-H}}$ are quite complicated [7], the programs SCHOONSCHIP [10] and FORM [11] were used to perform the algebraic manipulations. The explicit forms of the $T_{\lambda_1 \lambda_2 \lambda_3 \lambda_4}^i$ are given in Table II. In order to isolate the cutoff dependence, we introduce a renormalization scale μ and rewrite Eq. (15) as

$$T_{\lambda_1 \lambda_2 \lambda_3 \lambda_4}^{(2)} = \frac{\alpha^4}{(45\pi)^2} \frac{\omega^8}{m_e^8} \ln \left(\frac{\Lambda^2}{\mu^2} \right) \sum_{i=s,t,u} T_{\lambda_1 \lambda_2 \lambda_3 \lambda_4}^i + \tilde{T}_{\lambda_1 \lambda_2 \lambda_3 \lambda_4}^{(2)}, \quad (16)$$

where $\tilde{T}_{\lambda_1 \lambda_2 \lambda_3 \lambda_4}^{(2)}$ is obtained from Eq. (15) by replacing Λ^2 with μ^2 in B_0 . The sums of the various helicity combinations are given in the last row of Table II.

To complete the interpretation of the cutoff-dependent terms in Eq. (16) as contributions to coupling constant renormalization, it is necessary to show that they can be obtained as matrix elements of local, gauge invariant operators. The operators occurring in Eq. (10) are sufficient, and we find

$$\mathcal{L}_{\text{E-H}}^{(2)} = \frac{1}{10(90\pi)^2} \frac{\alpha^4}{m_e^8} \ln\left(\frac{\Lambda^2}{\mu^2}\right) \left\{ 182 (\partial_\alpha F_{\mu\nu})(\partial^\alpha F^{\mu\nu})(\partial_\beta F_{\lambda\rho})(\partial^\beta F^{\lambda\rho}) \right. \\ \left. - 639 (\partial_\alpha F_{\mu\nu})(\partial^\beta F^{\mu\nu})(\partial^\alpha F_{\lambda\rho})(\partial_\beta F^{\lambda\rho}) + 1523 (\partial^\alpha \partial_\beta F_{\mu\lambda}) F^{\lambda\nu} (\partial^\mu \partial_\nu F_{\alpha\rho}) F^{\rho\beta} \right\}. \quad (17)$$

The effective Lagrangian

$$\mathcal{L} = \mathcal{L}_{\text{E-H}} + \frac{1}{m_e^8} \left\{ a_1 (\partial_\alpha F_{\mu\nu})(\partial^\alpha F^{\mu\nu})(\partial_\beta F_{\lambda\rho})(\partial^\beta F^{\lambda\rho}) \right. \\ \left. + a_2 (\partial_\alpha F_{\mu\nu})(\partial^\beta F^{\mu\nu})(\partial^\alpha F_{\lambda\rho})(\partial_\beta F^{\lambda\rho}) + a_3 (\partial^\alpha \partial_\beta F_{\mu\lambda}) F^{\lambda\nu} (\partial^\mu \partial_\nu F_{\alpha\rho}) F^{\rho\beta} \right\} \quad (18)$$

then gives a finite matrix element for elastic scattering at the one-loop level provided the cutoff dependent terms represented by Eq. (17) are interpreted as renormalizations of the coupling constants a_1 , a_2 and a_3 .

IV. DISCUSSION

As shown in Section II, the low energy photon-photon scattering amplitude in QED can be expanded in powers of ω^2/m_e^2 , beginning with a term of order ω^4/m_e^4 . The first three terms of this expansion, given by Eqs. (2,4,5), are reproducible using the matrix elements of the local interactions Eqs. (8-10). On the other hand, using the Euler-Heisenberg expansion, Eq. (11), to the one-loop level in perturbation theory results in an effective interaction in which there is no contribution to the elastic amplitude of order ω^6/m_e^6 . Therefore, it is not necessary to introduce a counterterm to ensure renormalizability in this order. An ω^6/m_e^6 correction cannot be generated by retaining more terms in the Euler-Heisenberg expansion or by including perturbative corrections with more than one loop. We do obtain finite one-loop terms of order ω^8/m_e^8 , but these are higher order in α than Eq. (10) and thus should be negligible numerically. In fact, the discussion in Section III is essentially complete with regard to corrections of order ω^8/m_e^8 . The only other potential ω^8 correction to the elastic amplitude is associated with term in the Euler-Heisenberg expansion which consists of products of eight field tensors, but this contribution also vanishes by dimensional regulation.

There is thus a difference between the energy dependence derived from QED and that implied by simply requiring the renormalizability of the effective Lagrangian approach. This fact does not seem to be in conflict with the spirit of effective field theory, since one can always add interactions such as those in Eq. (9) to recover the ω^6 dependence. One cannot, however, restrict the number of such terms by appealing to renormalizability.

ACKNOWLEDGMENTS

We thank Vic Teplitz, Steven Weinberg and Scott Willenbrock for discussions. This research was supported in part by the U. S. Department of Energy under Grant No. DE-FG02-95ER40896, DE-FG013-93ER40757, in part by the National Science Foundation under

Grant No. PHY-93-07780 and in part by the University of Wisconsin Research Committee with funds granted by the Wisconsin Alumni Research Foundation.

REFERENCES

- [1] R. Karplus and M. Neuman, Phys. Rev. **80**, 380 (1950).
- [2] B. DeTollis, Nuovo Cim. **35**, 1182 (1965).
- [3] H. Euler, Ann. Phys. (Leipzig) **26**, 398 (1936); W. Heisenberg and H. Euler, Zeit. Phys. **98**, 714 (1936).
- [4] C. Kao and D.A. Dicus, LOOP, a Fortran program for evaluating loop integrals based on the following two papers: G. t'Hooft and M. Veltman, Nuc. Phys B **153**, 365 (1979), and G. Passarino and M. Veltman, Nuc. Phys. B **160**, 151 (1979).
- [5] F. Ravndal, *Applications of Effective Lagrangians*, hep-ph/9708449; V. I. Ritus, Proc. Lebed. Phys. Inst. **168**, Nova Science Pub., New York, N.Y. (1986); M. Reuter, M. G. Schmidt and C. Schubert, hep-th/9610191 (1996).
- [6] S. Weinberg, Physica **96A**, 327 (1979); Proc. of the XXVI International Conference on High Energy Physics, edited by J. R. Sanford, AIP Press (1993), p. 352; University of Texas Theory Group report UTTG-05-97, hep-th/9702027 (1997).
- [7] A first try along these lines was made by J. Halter, Phys. Lett. B **316**, 155 (1993). Note that the vertex function $\mathcal{M}^{\alpha\beta\mu\nu}$ given in the Appendix contains a misprint: the first terms in lines 7, 9, 11, 13, 15 and 17 should not be multiplied by 2.
- [8] The Euler-Heisenberg Lagrangian is an expansion in powers of the field tensor $F_{\mu\nu}$ which takes the form $(eF)^{2n+2} m_e^{-4n}$, where e is the electric charge and $n = 1, 2, 3, \dots$.
- [9] In this paper, we consider only elastic scattering, $\gamma\gamma \rightarrow \gamma\gamma$. The second term in Eq. (11) gives the low energy ($\omega < m_e$) contribution to $\gamma\gamma \rightarrow 4\gamma$. The total cross section for the inelastic process $\gamma\gamma \rightarrow 4\gamma$ is $\sigma^{(6)} = 8.0 \times 10^{-40} (\omega/m_e)^{14} \text{ cm}^2$. This can be compared to Eq. (3), which gives $\sigma^{(4)} = 1.3 \times 10^{-31} (\omega/m_e)^6 \text{ cm}^2$.
- [10] M. J. G. Veltman, *SCHOONSCHIP A Program for Symbol Handling*, University of Michigan, report, 1984 (unpublished).
- [11] J. A. M. Vermaseren, *The Symbolic manipulation program FORM*, Report No. KEK-TH-326, 1992 (unpublished).

TABLES

ω	σ	R_1	R_2
0.25	3.20×10^{-35}	0.983	1.001
0.35	2.46×10^{-34}	0.966	1.010
0.45	1.15×10^{-34}	0.931	1.020
0.55	4.08×10^{-33}	0.876	1.036
0.65	1.22×10^{-32}	0.799	1.054
0.75	3.32×10^{-32}	0.692	1.054
0.85	9.07×10^{-32}	0.537	0.977
0.95	3.02×10^{-31}	0.314	0.701
0.99	6.74×10^{-31}	0.180	0.438
1.00	1.26×10^{-30}	0.102	0.255

TABLE I. The first column gives the photon center-of-mass energy in units of the electron mass. The second column is the full one loop cross section, as calculated numerically, in cm^2 . This is the same cross section as in Fig. 1. The third column is the ratio of the approximate cross section (3) to the full cross section in column 2. The fourth column is the ratio of the improved cross section (7) to the full cross section.

	+++	+-	+-
$T_{\lambda_1 \lambda_2 \lambda_3 \lambda_4}^s$	$\frac{8}{5}(1459 + 3z^2)$	-1760	$\frac{968}{5}(1+z)^2$
$T_{\lambda_1 \lambda_2 \lambda_3 \lambda_4}^t$	$\frac{968}{5}(1-z)^2$	$-110(1-z)^4$	$\frac{242}{5}(1-z^2)^2$
$T_{\lambda_1 \lambda_2 \lambda_3 \lambda_4}^u$	$\frac{968}{5}(1+z)^2$	$-110(1+z)^4$	$\frac{1}{5}(1+z)^2(743 + 1450z + 731z^2)$
$\sum_{s,t,u} T_{\lambda_1 \lambda_2 \lambda_3 \lambda_4}^i$	$\frac{8}{5}(1701 + 245z^2)$	$-220(3+z^2)^2$	$\frac{1}{5}(1+z)^2(1953 + 966z + 973z^2)$

TABLE II. The contributions to the helicity amplitudes of Eq. (15) from the Euler-Heisenberg Lagrangian used to one-loop are given in the first three rows. In addition, $T_{+--+}^s(z) = T_{+--+}^s(-z)$ while $T_{+--+}^t(z) = T_{+--+}^t(-z)$, $T_{+--+}^u(z) = T_{+--+}^u(-z)$ and $T_{++++}^i(z) = T_{++++}^i(z) = 0$ for $i = s, t, u$. The last row is the sum needed in Eq. (16).

FIGURES

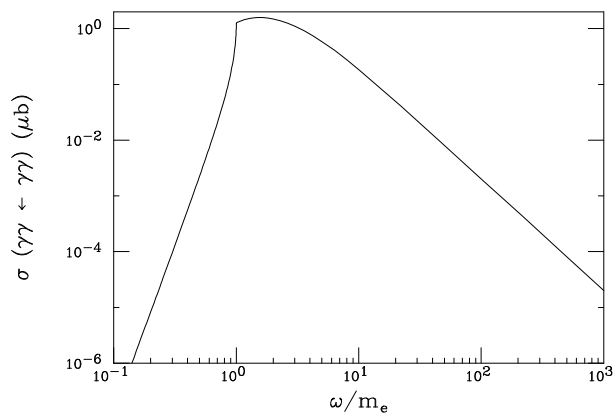


FIG. 1. The exact cross section for $\gamma\gamma \rightarrow \gamma\gamma$ is shown.

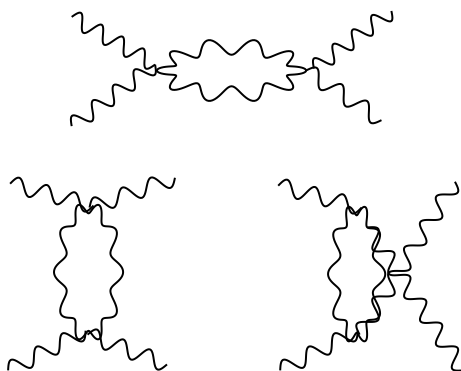


FIG. 2. One-loop diagrams for the s , t and u channel two photon exchanges are shown.